Preliminary Analysis on the Use of a Process-Based Forest Growth Model of *Cryptomeria japonica* Planted Forest to Represent the Effects of Canopy Structure Change

Mitsuda, Y., Hosoda, K., Iehara, T. & Matsumoto, M.

Keywords: Process-based model, light-curve, canopy structure, *Cryptomeria japonica*, Bayesian calibration

Abstract: The objective of this study is to modify the process-based stand growth model for *Cryptomeria japonica* in the photosynthetic production process so as to more reasonably represent the stand growth pattern after thinning. We introduce five leaf strata to the canopy structure, and then parameterize the light-curve for each leaf stratum by Bayesian calibration via the Markov Chain Monte Carlo (MCMC) method. We examine the behavior of the model using the estimated light-curve parameters through a simulation approach. We used the forest stand data derived from repeated measurements of three permanent plots. The posterior distribution of light-curve parameters derived from MCMC were well converged. We virtually applied three thinning scenarios, upper thinning, random thinning and lower thinning, and then simulated stand growth. The modified model could well reflect the changes in canopy structure derived from thinning on the growth pattern after thinning. The results suggest that the multiple light-curve model adopted in this study would be represent more realistic stand dynamics after thinning than single light-curve model adopted in the former model.

Received September 9, 2010; Accepted December 29, 2010

1 Introduction

Accounting for carbon stock and its flux in forests is an important issue in the forest sector as carbon sequestration by forests can mitigate the increase in atmospheric CO_2. The carbon sequestration rate in forest stands is determined not only by climatic and edaphic factors, but also by forest management regimes (e.g. Mäkipää *et al.*, 1999, Mäkelä *et al.*, 2000, Lasch *et al.*, 2005). Because appropriate forest management is recognized as an effective method for facilitating carbon sequestration under the Kyoto Protocol (Sedjo *et al.*, 2002, IPCC 2003, Hiroshima and Nakajima, 2006), there is an urgent to develop an effective forest management regime to enhance carbon sequestration by forests. Thus, the importance of predicting forest growth under changing climatic conditions and various forest management regimes has been increasing.

Process-based models (PBMs) include physiological interactions between plants and their environment, and are thus suitable for use with predicted future climate conditions, and they are also suitable for simulating the effects of various management regimes (e.g. combinations of timing and intensity of thinning) on stand growth. A number of process-based forest growth models have been developed to better understand the carbon cycle of forest ecosystems (e.g. Gertner *et al.*, 1996, Landsberg and Waring, 1997, Chiba, 1998, Kurz and Apps, 1999, Mäkelä *et al.*, 2000, Dufrêne *et al.*, 2005). We have developed a process-based stand growth model for *Cryptomeria japonica* (Mitsuda *et al.*, 2010), which is the dominant planting species in Japan. Planted forests of *Cryptomeria japonica* account for approximately 18% of the entire forest area of Japan; therefore, it is important to develope reliable tools for improving the forest management of this species.

Our model is based on the 3-PG (Physiological Principles Predicting Growth) model developed by Landsberg and Waring (1997). In the previous study, we simplified the model so as to have only two cli-

matic factors restricting the potential gross photosynthetic rate. At the same time, we modified the calculation method for the potential gross photosynthetic rate. In the original 3-PG model, absorbed solar radiation is converted to gross primary production using constant canopy quantum efficiency. However, we used a light-response curve to express the nonlinear relationship between photosynthetic rate and intensity of absorbed radiation (e.g. Hirose and Werger, 1987).

In this study, we intended to modify the photosynthetic production process from the former model to more accurately represent the stand growth pattern after thinning. It is well known that the shape of the light-response curve changes with relative height in the canopy (e.g. Hirose and Werger, 1987). Higher reliability of predictions, which is an advantage of PBMs, is assured by the fact that PBMs contain ecophysiological processes. Including advanced knowledge about the ecophysiological response in plant photosynthesis into PBMs should improve its reliability. Therefore, we aimed to modify the monomorphic light-response curve to a polymorphic light-response curve that changes with relative height in the canopy. We introduced five leaf strata to the canopy structure, and then calculated the intensity of radiation, related photosynthetic rate using the polymorphic light-curve, and gross primary production for each leaf stratum. This modification will allow us to evaluate the effects of different thinning scenarios on stand growth.

2 Materials and methods

2.1 Model

The 3-PG model is a simple but powerful process-based, stand-level model of forest growth (Landsberg and Waring, 1997, Sands and Landsberg, 2002), which has been developed for several species in different regions (e.g. Esprey *et al.*, 2004, Fontes *et al.*, 2006). In the previous

study, we modified the 3-PG model to a simpler version having only six processes: (1) photosynthetically active radiation absorption; (2) photosynthetic production; (3) constraints on photosynthesis by environmental factors; (4) respiration; (5) litterfall and root turnover; and (6) biomass partitioning (Figure 1). The photosynthesis part of the 3-PG model, which includes processes (1) and (2), is based on the Monsi-Saeki canopy photosynthesis model. We used a monthly time-step for calculating photosynthesis, yearly time-step for calculating respiration and litterfall, and biomass partitioning. Dry matter weight per unit area of four biomass pools (i.e. foliage, stem, branch, and root) was used as the basis for calculating the carbon balance. All parameters, inputs, and outputs of our model and associated symbols are listed in Table 1.

Hereafter, we briefly describe the model structure and how we mod-

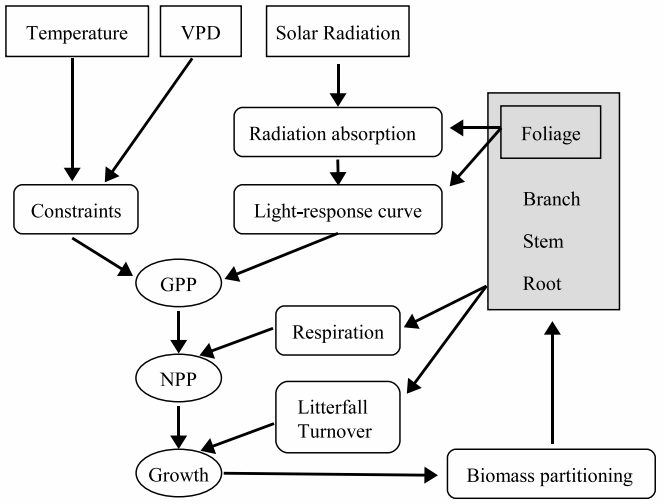

Figure 1. Flow diagram of the carbon cycle model developed in this study.

Table 1. Inputs and main outputs of the stand growth model.

	Meaning	Symbol	Unit
Inputs			
	Total short-wave incoming radiation	ϕ_s	MJ/ha/month
	Monthly mean temperature	T	°C
	Monthly mean VPD	D	kPa
Inputs/outputs			
	Foliage biomass	W_f	ton/ha
	Branch biomass	W_b	ton/ha
	Stem biomass	W_s	ton/ha
	Root biomass	W_r	ton/ha
Outputs			
	GPP	P_G	ton/ha/year
	NPP	P_N	ton/ha/year
	Total biomass growth	G_B	ton/ha/year
	Respiration	R	ton/ha/year
	Litterfall	L	ton/ha/year

ified this model in this study.

2.1.1 Photosynthetically active radiation absorption

Photosynthetically active radiation absorbed by foliage (APAR, ϕ_{pa}) is calculated by Beer's law;

$$[1] \qquad \phi_{pa} = \phi_p(1 - \exp(-K\,W_f))$$

where K is the light-extinction coefficient, ϕ_p is photosynthetically active radiation (PAR) assumed to be half of the total shortwave incoming radiation (ϕ_{ps}), and W_f is foliage biomass. Units of variables are shown in Table 1. Beer's law is primarily applied using the leaf area index (LAI); however, as described later, we utilized the biomass of each part as input data, and since we did not have an adequate conversion equation, we substituted foliage biomass for LAI.

2.1.2 Photosynthetic production

In the original 3-PG model, APAR is converted to gross primary production (GPP) using canopy quantum efficiency, which was set to be constant, whereas we used the gross photosynthetic rate to express the nonlinear relationship between light-use efficiency and intensity of APAR. To represent this nonlinear relationship, we adopted a nonrectangular hyperbola, which is often used for the light-response curve of canopy photosynthesis (e.g. Hirose and Werger 1987).

$$[2] \qquad A_G = \frac{aI + A_{max} - \sqrt{(aI + A_{max})^2 - 4aI\theta A_{max}}}{2\theta}$$

$$[3] \qquad I = \frac{\phi_{pa}}{W_f}$$

where A_G is the gross photosynthetic rate per unit foliage weight (ton/ton), A_{max} is the light-saturated gross photosynthetic rate, a is the initial slope of the light-response curve, θ is the convexity of the light-response curve, and I is the APAR per unit foliage weight. Units of variables are shown in Table 1.

Modification

In this study, we modified this single light-curve model used in the previous model to a multiple light-curve model, which had an individual parameter A_{max} for each stratum parameterized as follows:

$$[4] \qquad A_{max,i} = \alpha_i \, A_{max,i-1} \quad i = 2, 3, 4, 5$$

where α means the coefficients and subscript i means layer of canopy stratum from top (1) to bottom (5). The light-saturated gross photosynthesis rate gradually decreases from the canopy top to bottom; therefore, this parameter for layer 1 ($A_{max,1}$) is not penalized, and the parameters for the lower layers are reduced by parameter α_i ranging

from 0 to 1.

To examine the effect of model modification, we compared the previous single light-curve model and the newly developed multi-curve model by a growth simulation with various thinning scenarios.

2.1.3 Environmental constraints on photosynthesis

We used only two environmental constraints: temperature and vapor pressure deficit (VPD), because they are major limiting factors of forest stand growth (e.g. Shidei and Kira, 1977), and their data can be easily acquired.

Generally, temperature directly affects the biochemical reaction of photosynthesis, and photosynthetic activity falls drastically at lower temperature (Hikosaka *et al.*, 2006). For *Cryptomeria japonica*, temperature is also a determining factor for growth and natural distribution (Mashimo, 1983). VPD, which controls canopy conductance and photosynthetic rate as a result (e.g. Landsberg and Waring, 1997), is known as one of the dominant growth limiting factors for *Cryptomeria japonica* (e.g. Shigenaga *et al.*, 2005). In the 3-PG model, environmental constraints on photosynthesis were included as growth modifiers, the values of which ranged from 0 to 1. The temperature modifier (f_T) and VPD modifier (f_D) are described as follows:

$$[5] \qquad f_T = \frac{1}{1 + \exp(-k_{T1}(T - k_{T2}))}$$

$$[6] \qquad f_D = \exp(-k_D D)$$

where T and D are monthly mean temperature and monthly mean VPD (units are shown in Table 1, respectively, and k_{T1}, k_{T2}, k_D are coefficients. In our model, f_T and f_D act as growth limiting factors for low temperature in winter and water stress in summer, respectively

respectively (Mitsuda *et al.*, 2010).

Thus, the monthly GPP of a stand was calculated as the product of the temperature modifier, VPD modifier, and gross photosynthetic rate multiplied by the foliage weight as follows:

$$[7] \qquad P_g = f_T f_D A_G W_f$$

The yearly GPP (P_G) is the sum of the monthly GPP (P_g).

2.1.4 Respiration and Turnover

Respiration of each biomass pool was calculated in proportion to its biomass using a yearly time-step (Chiba, 1998). Litterfall and root turnover were calculated as well.

$$[8] \qquad R_j = r_j W_j$$

$$[9] \qquad L_j = h_j W_j$$

where R_j and L_j are respiration and litterfall (or root turnover), respectively, r_j and h_j are their its respective rates per unit biomass (ton/ton), and W_j is biomass (ton/ha). Subscript j means each biomass pool as f for foliage, s for stem, b for branch, and r for root. Units of variables are shown in Table 1.

Thus, yearly net primary production (NPP, P_N) and total biomass growth (G_B) were calculated as follows:

$$[10] \qquad P_N = P_G - \sum_{i \in (f,s,b,r)} R_i$$

$$[11] \qquad G_B = P_N - \sum_{i \in (f,s,b,r)} L_i$$

Modification: Here, we also modified foliage respiration to take into consideration the change in light-response curve along with canopy height. The respiration of foliage in the middle layer (i.e. layer 3) was regarded as the baseline, and its annual rate per unit foliage weight was set at 1.8 (ton/ton/year) derived from the previous study (Chiba, 1998). For the other layers, we adjusted the respiration rate using parameter α_i introduced to represent the change in light-saturated gross photosynthesis rate with canopy height (Eq. [4]). Thus, the respiration rate for each canopy layer is described as follows:

[12] $$r_{f,1} = r_{f,3}/\alpha_2/\alpha_3$$

[13] $$r_{f,2} = r_{f,3}/\alpha_3$$

[14] $$r_{f,3} = 1.8$$

[15] $$r_{f,4} = r_{f,3}\,\alpha_4$$

[16] $$r_{f,5} = r_{f,3}\,\alpha_4\,\alpha_5$$

where $r_{f,i}$ means the respiration rate of the foliage in layer i. Since parameters α_i range from 0 to 1, $r_{f,1}$ must take the largest value and decrease gradually to $r_{f,5}$.

2.1.5 Growth partitioning

Total biomass growth was partitioned into four biomass pools. We already had the biomass proportion functions for *Cryptomeria japonica* that describe the relationship between tree age and proportion of biomass of each pool (Fukuda *et al.*, 2003), from which we derived the biomass growth partitioning function.

2.2 Data

We used the forest stand data derived from repeated measurements

of three permanent plots (Iehara *et al.*, 2001). A summary of the yield plots is shown in Table 2. Diameter at breast height (1.2 m) was measured for all standing trees, and tree height was measured for selected trees at earlier measurements or all standing trees at later measurements. Unmeasured tree height was estimated using the relationship between diameter and height of measured trees of the same plot and measurement. Since we already had the tree volume equations for major species in Japan (Forest Planning Section, Japan Forestry Agency 1970), we could calculate the single-tree volume using diameter and height. We introduced the basic wood density of *Cryptomeria japonica*, which was 0.314 g/cm^3 (Greenhouse Gas Inventory Office of Japan *et al.*, 2008), and obtained the stem biomass of each tree by multiplying the basic wood density by tree volume, and then we calculated the biomass of the other pools using the biomass partitioning function (Fukuda *et al.*, 2003). The biomass of each tree was summed up to obtain the stand-level biomass.

We estimated time-series climatic values for monthly solar radiation, mean temperature, and vapor pressure deficit (VPD) for the entire measurement period using the 30-year average values at 1-km resolution published by Japan Meteorological Agency (2002) and the climatic data of the nearest meteorological stations for the plots.

An example of a time-series of stem biomass and climatic values is shown in Figure 2.

2.3 Parameterization

Bayesian calibration via the Markov Chain Monte Carlo (MCMC) method that yields a sample of values from the posterior distribution of parameters (conditioned parameter distribution for measured data) was applied for parameterization of our model. In this study, we parameterized only parameters $A_{max,1}$ and α_i appearing in Eq. [4] and Eqs

Table 2. Summary of the permanent plot data.

Plot	Age	DBH	Height	Volume
1	11	8.8	6.4	90.3
	16	11.5	8.8	197.1
	21	15.2	10.8	224.3
	25	16.7	11.5	283.2
	31	17.9	13.5	385.9
	36	20.4	14.9	381.5
	46	23.4	17.9	602.1
	51	25.7	19.4	537.7
2	60	21.7	20.3	869.3
	69	23.7	21.9	1001.3
	79	25.4	23.2	1109.4
	89	27.7	23.8	1076.9
3	46	20.9	15.8	383.9
	51	21.6	16.2	412.6
	60	25.0	17.0	553.6
	72	26.2	17.8	616.6
	81	28.3	19.5	779.3
		(cm)	(m)	(m^3/ha)

[12] to [16] and the other parameters were set as constants derived from previous studies (Tadaki *et al.*, 1965 1967, Tadaki and Hatiya, 1968, Chiba 1998, Mitsuda *et al.*, 2010). The values of fixed parameters are listed in Table 3.

Since the permanent plot data was derived from repeated measurements, the effect of the difference among plots, which means unmeasured differences in genetic variation, soil fertility, soil water holding capacity, and soil water bodies among plots, should be considered; therefore we introduced a hierarchical structure in the parameterization. The parameter $A_{max,1}$ of the multiple light-curve model was redefined as a common parameter for all plots, and plot-level parameters $A'_{max,1_k}$ for each plot k were introduced to the light-response curve (Eq.

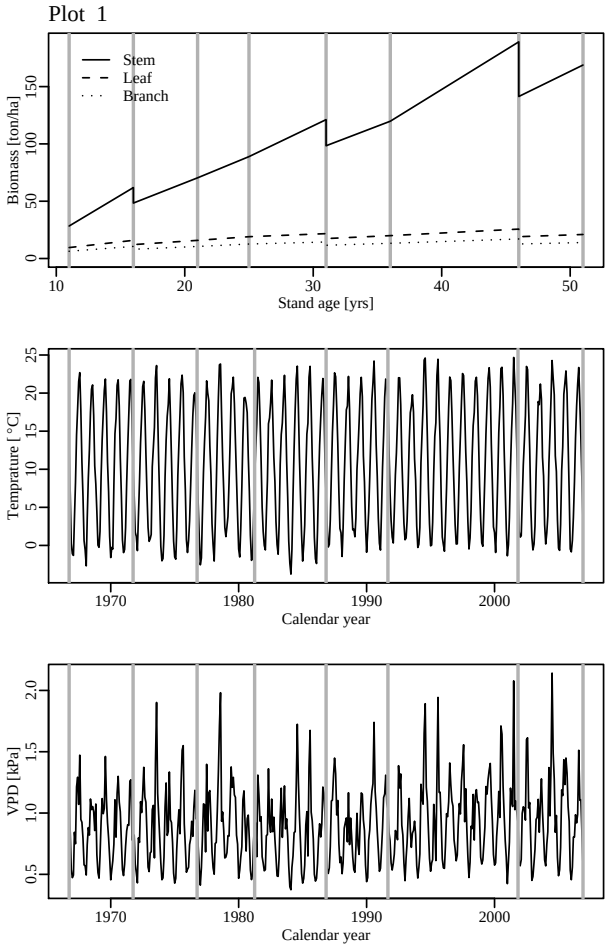

Figure 2. Example of time-series of stem biomass and climatic values for a plot.

[2]). The plot-level parameters $A'_{max,1_k}$ were assumed to be distributed normally with mean = $A_{max,1}$ and standard deviation = $\sigma_{A_{max}}$, which was also estimated through Bayesian calibration. For a comparison, we

Table 3. Posterior distribution of model parameters and values of fixed parameters.

Estimated parameters					
Symbol	Mean	Median	SD	$\hat{R}$	
$A_{max,1}$	1.05	1.03	0.21	1.00	
$A'_{max,1_1}$	0.92	0.92	0.03	1.05	
$A'_{max,1_2}$	1.62	1.61	0.09	1.02	
$A'_{max,1_3}$	0.71	0.71	0.03	1.01	
α_2	0.90	0.90	0.01	1.12	
α_3	0.89	0.90	0.01	1.05	
α_4	0.49	0.49	0.02	1.03	
α_5	0.49	0.49	0.03	1.19	
Fixed parameters					
Symbol	Value				
K	0.15	r_f	1.8	h_f	0.222
a	10.0	r_b	0.035	h_b	0.171
θ	0.9	r_s	0.035	h_s	0.0002
k_{T1}	0.3	r_r	0.035	h_r	0.07
k_{T2}	5.0				
k_D	0.5				

Variable names are given in the text.

also adopted this hierarchical structure for the single light-curve model and introduced a common parameter A_{max} and plot level parameter A'_{max_k} for each plot k.

We defined the likelihood function as the distribution of measurement errors in total biomass assuming Gaussian distribution with mean = 0 and standard deviation = σ_E. In this study, σ_E was fixed as the value of the standard deviation in observed total biomass.

$$[17] \qquad \begin{aligned} P(Data|Parameters) &= P(E = O - M) \\ &= L(E|A_{max,1}, \alpha_{2,3,4,5}, \sigma_{A_{max}}, A_{max,1_k}) \end{aligned}$$

[18] $E \sim N(0, \sigma_E^2)$

where E is measurement error, and O and M are observed and model output values, respectively, for total biomass.

Since parameter α_i range from 0 to 1, we adopted the logit transformation to this parameter. Then, the prior distribution of parameters of transformed α_i and also $A_{max,1}$ was set as the normal distribution with mean = 0 and standard deviation = 100. For the standard deviation parameter (i.e. $\sigma_{A_{max}}$), we used noninformative Gamma prior distribution. Bayesian calibration via the MCMC method was conducted using WinBUGS (Spiegelhalter *et al.*, 1996). We ran three parallel MCMC chains for 300,000 iterations, and dropped the first 290,000 iterations as the "burn-in" period.

2.4 Simulation

Using the estimated parameters, we predicted stand growth using various thinning scenarios. Since plot 2 was not thinned, we selected the first measurement of plot 2 as the initial stand status for the thinning simulation. We virtually applied three thinning scenarios, upper thinning (UT), random thinning (RT) and lower thinning (LT), under the same stand volume removal rate as 20%. The DBH distribution after thinning is shown in Figure 3. We predicted the growth of stands to which each thinning scenario was applied for the period from the first to second measurement.

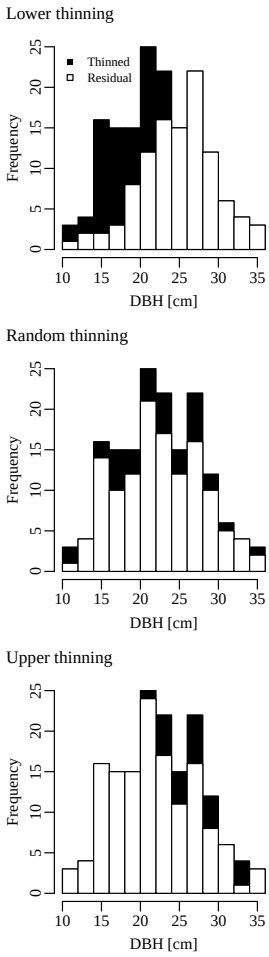

Figure 3. Diameter distribution after thinning implementation.

3. Results and Discussion

From the density diagrams of the samples from the posterior distribution of $A_{max,1}$, plot-level parameters $A'_{max,1_k}$ derived from MCMC, we could see their sharply peaked distribution, which indicated that

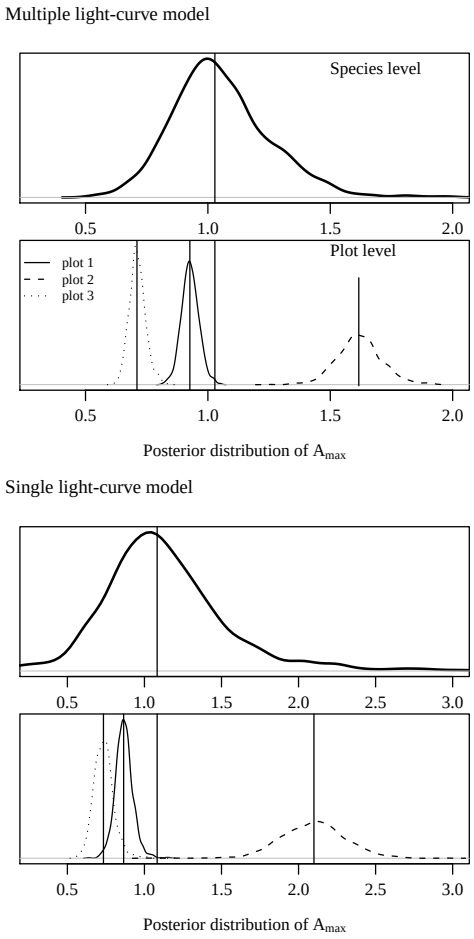

Figure 4. Density diagrams of samples from the posterior distribution of parameter of the lightsaturated gross photosynthetic rate.

these parameters were well conditioned by the data (Figure 4). Also, parameters A_{max} and A'_{max_k} of the single light-curve model were well conditioned. The mean, median, and standard deviation of samples from the posterior are shown in Table 3. The convergence diagnos-

tics ($\hat{R}$) developed by Gelman and Rubin (1992) was below 1.2 for all parameters (Table 3), which indicates that all parameters were well converged through the Bayesian calibration (Gelman *et al.*, 2003)

Comparing the plot-level parameters $A'_{max,1_k}$, the parameter for plot 2 was larger than that for the other two plots. Since plot 2 was unthinned and relatively old aged, its density was quite high at each measurement, a large part of the trees had been suppressed and inhibited radial growth. Suppressed trees tend to be thin relative to their height and have less leaf biomass. Since the biomass partitioning function that we applied to these suppressed trees was originally developed for normal trees (Fukuda *et al.*, 2003), the stand leaf biomass of plot 2 might be overestimated. This overestimated leaf biomass would have resulted in the overestimation of leaf respiration, and to compensate for higher respiration, the light-saturated gross photosynthetic rate of plot 2 ($A'_{max,1_2}$) must be estimated at a higher value than that of the other plots. The estimation of root, stem, branch and leaf biomass from measured tree size (i.e. DBH and H) is the basis for carbon cycle modeling; therefore, we should improve the method for this estimation so that consideration is given to the varying proportion of each biomass pool among the trees. The biomass partitioning function used in this study is an empirical model; however, a theoretical approach might be preferable (e.g. Mäkelä *et al.*, 1997).

For the comparison between the single light-curve model and multiple light-curve model, we conducted virtual thinning simulations. Medians of each sample from the posterior distribution were used as estimates of each parameter. Time series of the simulated total biomass and measured total biomass, which is indicated as the biomass growth pattern in the case without thinning (denoted as 'Unthinned'), are compared in Figure 5. Furthermore, we calculated the leaf production efficiency as annual NPP divided by leaf biomass for comparing these two models in

detail (Fig.6). The volume removal rate was the same for the three thinning scenarios, although the growth rate and leaf production efficiency were different. This result reflects the changes in canopy structure derived from thinning. Since leaves in the upper canopy were removed by thinning, the light intensity in the lower canopy increased and the photosynthesis rate of the lower canopy improved. Since leaves in the lower canopy were removed by thinning, the carbon balance between photosynthesis production and respiration of whole canopy improved. Applying lower thinning removed much more leaves from lower canopy than other thinning, as a result, leaf production efficiency after lower thinning improved at the highest rate among the three thinning scenarios. This result depends on the balance between photosynthesis production and respiration, and both physiological processes are restricted by several climatic conditions. In our model, however, only photosynthesis was controlled by climatic factors. Therefore, we cannot conclude that lower thinning is the most effective thinning scenario for improving leaf production efficiency.

Comparing the results from the single and multiple light-curve models, the biomass growth rate and leaf production efficiency predicted with the single light-curve model were higher than that with the multiple light-curve model (Fig.5 and 6). This result is due to the difference in the photosynthesis rate in the lower canopy, where the radiation intensity increased by the removal of leaves from the upper canopy. The actual light-saturated gross photosynthetic rate should be lower in the lower canopy because of the shortage of leaf nitrogen component (e.g. Hirose and Werger, 1987). Therefore, the calculated growth rate and leaf production efficiency derived from the single light-curve model might be higher than the actual values. The results of this study suggest that the multiple light-curve model would be able to represent more realistic stand dynamics after thinning. In this preliminary anal-

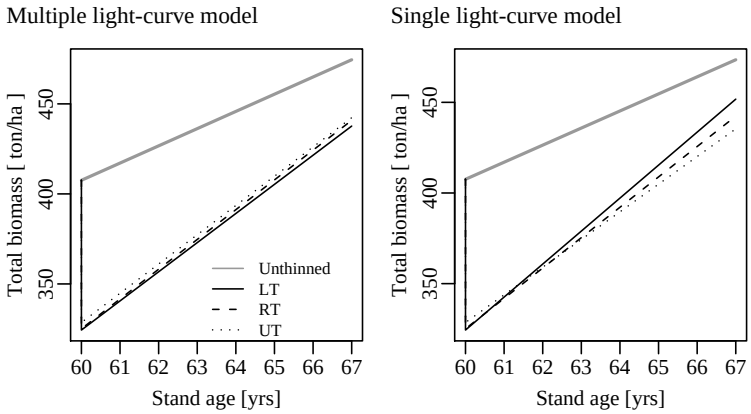

Figure 5. Simulated total biomass growth after thinning.

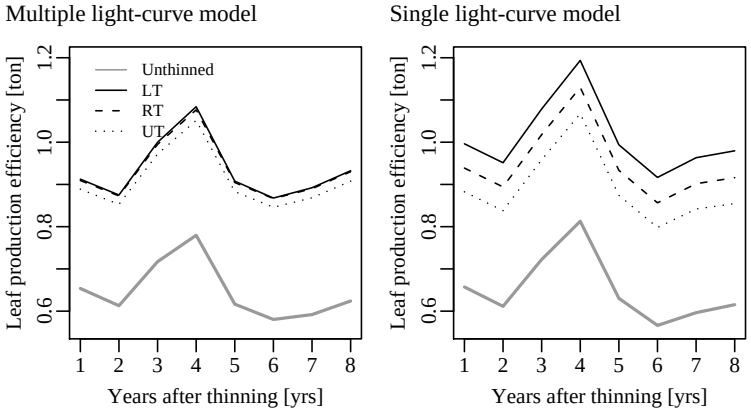

Figure 6. Simulated leaf production efficiency after thinning.

ysis, we used stand data acquired from only 3 plots; therefore, we need to examine these results using other data.

4. Conclusion

We successfully parameterized the multiple light-curve model for

the five leaf strata, which constituted our process-based stand growth model for *Cryptomeria japonica*. The results of thinning simulations suggested that the biomass growth and leaf production efficiency predicted by the multiple light-curve model were more consistent with the theory of ecophysiology than those predicted by the single light-curve model. However, our modified growth model contains several parts which should be represented by a more theoretical approach. Especially, the respiration process, which greatly affects leaf production efficiency, should include the effect of temperature. In this preliminary analysis, we conclude that we improved our process-based stand growth model for *Cryptomeria japonica* in terms of the ecophysiology of photosynthesis, but we cannot conclude that our model is a more reliable tool for forest management.

We will strive to improve our model both theoretically and using more field data in order to make it more reliable for improving forest management.

References

Chiba, Y. (1998) Simulation of CO_2 budget and ecological implications of sugi (*Cryptomeria japonica*) man-made forests in Japan, *Ecol. Model.* 111(2-3):269–281.

Dufrêne, E., Davi, H., François, C., le Maire, G., Dantec, V. L. and Granier, A. (2005) Modelling carbon and water cycles in a beech forest: Part I: Model description and uncertainty analysis on modelled NEE, *Ecol. Model.* 185(2-4):407–436.

Esprey, L. J., Sands, P. J. and Smith, C. W. (2004) Understanding 3-PG using a sensitivity analysis, *Forest Ecol. Manag.* 193(1-2):235–250.

Fontes, L., Landsberg, J., Tomé, J., Tomé, M. and *et al.* (2006) Calibration and testing of a generalized process-based model for use in

portuguese eucalyptus plantations, *Can.J. Forest Res.* 36(12):3209–3221.

Forest Planning Section, Japan Forestry Agency (1970) *Tree volume table for eastern Japan*, Japan Forestry Investigation Comittee, Tokyo, Japan.

Fukuda, M., Iehara, T. and Matsumoto, M. (2003) Carbon stock estimates for sugi and hinoki forests in japan, *Forest Ecol. Manag.* 184(1-3):1–16.

Gelman, A., Carlin, J. B., Stern, H. S. and Rubin, D. B. (2003) *Bayesian Data Analysis*, Chapman & Hall, Boca Raton, USA 2 edition.

Gelman, A. and Rubin, D. (1992) Inference from iterative simulation using multiple sequences, *Stat. Sci.* 7:457–511.

Gertner, G., Parysow, P. and Guan, B. (1996) Projection variance partitioning of a conceptual forest growth model with orthogonal polynomials, *Forest Sci.* 42:474–486.

Greenhouse Gas Inventory Office of Japan, Center for Global Environmental Research and National Institute for Environmental Studies, editors (2008) *National greenhouse gas Inventory report of Japan*, National Institute for Environmental Studies, Tsukuba, Japan.

Hikosaka, K., Ishikawa, K., Borjigidai, A., Muller, O. and Onoda, Y. (2006) Temperature acclimation of photosynthesis: mechanisms involved in the changes in temperature dependence of photosynthetic rate, *J. Exp. Bot.* 57(2):291–302.

Hirose, T. and Werger, M. J. A. (1987) Maximizing daily canopy photosynthesis with respect to the leaf nitrogen allocation pattern in the canopy, *Oecologia* 72(4):520–526.

Hiroshima, T. and Nakajima, T. (2006) Estimation of sequestered carbon in article-3.4 private planted forests in the first commitment period in japan, *J. Forest Res.* 11(6):427–437.

Iehara, T., Miyamoto, A., Fukuda, M., Nishizono, T., Sano, M. and Takahashi, M. (2001) *Stand structure and growth of yeild plots in Kanto district*, Forestry and Forest Products Research Institute.

IPCC (2003) *Good practice guidance for land use, land-use change and forestry*, IPCC National Greenhouse Gas Inventories Programme Technical Support Unit., Hayama, Kanagawa, Japan.

Japan Meteorological Agency (2002) *Mesh climate data for 1971–2000*, Japan Meteorological Business Suport Center.

Kurz, W. A. and Apps, M. J. (1999) A 70-year retrospective analysis of carbon fluxes in the Canadian forest sector, *Ecol. Appl.* 9(2):526–547.

Landsberg, J. and Waring, R. (1997) A generalised model of forest productivity using simplified concepts of radiation-use efficiency, carbon balance and partitioning, *Forest Ecol. Manag.* 95(3):209–228.

Lasch, P., Badeck, F., Suckow, F., Lindner, M. and Mohr, P. (2005) Model-based analysis of management alternatives at stand and regional level in brandenburg (Germany), *Forest Ecol. Manag.* 207(1-2):59–74.

Mäkelä, A., Landsberg, J., Ek, A. R., Burk, T. E., Ter-Mikaelian, M., Ågren, G. I., Oliver, C. D. and Puttonen, P. (2000) Process-based models for forest ecosystem management: current state of the art and challenges for practical implementation, *Tree Physiol.* 20(5-6):289–298.

Mäkelä, A., Vanninen, P. and Ikonen, V. (1997) An application of process-based modelling to the development of branchiness in scots pine, *Silv. Fenn.* 31(3):369–380.

Mäkipää, R., Karjalainen, T., Pussinen, A. and Kellomäki, S. (1999) Effects of climate change and nitrogen deposition on the carbon sequestration of a forest ecosystem in the boreal zone, *Can. J. Forest Res.* 29(10):1490–1501.

Mashimo, I. (1983) Relationship between growth and environmental factors for sugi plantation, In Sakaguchi, K., editor, *All about Sugi* Zenkoku Ringyo Fukyu Kyokai Tokyo, Japan.

Mitsuda, Y., Hosoda, K., Iehara, T. and Matsumoto, M. (2010) Parameterization of a process-based forest growth model using long-term yield survey plot data for predicting carbon sequestration in *Cryptomeria japonica* plantations, In Hoch, E. and Grunwald, S., editors, *Carbon Sequestration: Methods, Modeling and Impacts* Nova Science Publishers Inc New York, USA.

Sands, P.J. and Landsberg, J.J. (2002) Parameterisation of 3-PG for plantation grown eucalyptus globulus, *Forest Ecol. Manag.* 163(1-3):273–292.

Sedjo, R., Amano, M. and Yamagata, Y. (2002) The operationalization of the Kyoto Protocol with a focus on sinks :a perspective for Japan, *Bulletin of the Forestry and Forest Products Research Institute* 1:151–161.

Shidei, T. and Kira, T., editors (1977) *Primary productivity of Japanese forests; Productivity of terrestrial communities, JIBP synthesis*, University of Tokyo Press, Tokyo, Japan.

Shigenaga, H., Matsumoto, Y., Taoda, H. and Talahashi, M. (2005) The potential effect of climate change on the transpiration of sugi (*Cryptmeria Jjaponica* D. Don) plantations in Japan, *J. Agric. Meteorol.* 60:451–456.

Spiegelhalter, D., Thomas, A., Best, N. and Gilks, W. (1996) *BUGS: Bayesian Inference using Gibbs Sampling, Version 0.50.*

Tadaki, Y., Ogata, N. and Nagatomo, Y. (1965) The dry matter productivity in several stands of *Cryptomeria japonica* in Kushu, *Bulletin of the Goverment Forest Experiment Station* 173:45–66.

Tadaki, Y., Ogata, N. and Nagatomo, Y. (1967) Studies on production structure of forest. XI. Primary productivities of 28-year-old plan-

tations of *Cryptmeria* of cuttings and of seedlings origin, *Bulletin of the Goverment Forest Experiment Station* 199:48–65.

Tadaki, Y. and Hatiya, K. (1968) *Forest ecosystem and its dry matter production*, Ringyo Kagaku Gijutu Shinko-sha, Tokyo, Japan.

スギ人工林プロセスベース林分成長モデルにおいて林冠構造の変化が林分成長へおよぼす影響を表現するための予備的解析

光田　靖・細田和男・家原敏郎・松本光朗

要約: 本研究においてスギ人工林プロセスベース林分成長モデルを, 林冠構造の変化をとおして, 間伐後の成長をより合理的に表現できるように改良することを試みた。林冠構造に５層からなる階層構造を導入し, それぞれの葉群階層ごとに光―光合成曲線のパラメータを, マルコフ連鎖モンテカルロ法によるベイジアンキャリブレーションによって推定した。パラメータ推定に用いたのは長期固定試験地の継続調査によって得られた, 時系列の林分データである。推定の結果, 葉群階層ごとの光―光合成曲線パラメータはよく収束していた。また, 推定されたパラメータを利用して仮想的な間伐実験 (上層, 全層および下層間伐) を行い, モデルの挙動を検証した。シミュレーションの結果, 階層構造を導入したモデルは間伐による林冠構造の変化を上手く反映しており, 従来の単層モデルよりも合理的な成長予測が可能であることが示唆された。

キーワード: プロセスベースモデル・光―光合成曲線・林冠構造・スギ・ベイジアンキャリブレーション